Achieving Variable Compression Ratio By Opening Exhaust Valve During Compression Stroke

A THESIS PRESENTED
BY
SHELBIE L. DAVIS
TO
THE DEPARTMENT OF MECHANICAL ENGINEERING

IN PARTIAL FULFILLMENT OF THE REQUIREMENTS
FOR THE DEGREE OF
MASTER OF MECHANICAL ENGINEERING
IN THE SUBJECT OF
MECHANICAL ENGINEERING

SAINT MARTIN'S UNIVERSITY
LACEY, WASHINGTON
AUGUST 2017

Shelbie L. Davis, M.M.E. Candidate	Date
Frank M. Washko, Ph.D., J.D., Thesis Committee Chair	Date
Shawn Duan, Ph.D., Department Chair, Examiner	Date
Rico A.R. Picone, Ph.D., Examiner	Date

Thesis advisor: Professor Frank Washko Shelbie L. Davis

Achieving Variable Compression Ratio By Opening Exhaust Valve During Compression Stroke

Abstract

- The research in this paper serves as a proof-of-concept and feasibility analysis regarding variable compression ratio engine design utilizing an exhaust valve opening during the compression stroke to vary the compression ratio instead of the traditional method of changing the cylinder or piston geometry. A computational fluid dynamic model in ANSYS Forte was used to simulate a cold-flow, four-stroke, direct-injection engine cycle. For the first simulation trial, the compression ratio was 10 with one exhaust valve opening during the exhaust stroke. The result was a maximum cylinder pressure of 14.4 atm. For the following simulation trials, the compression ratio was increased to 17, and an additional valve opening at the end of the compression stroke was added. The additional valve opening profile was developed from the initial valve opening during the exhaust stroke. Timing of the additional valve opening was manipulated over multiple simulation iterations to finally achieve approximately the same maximum cylinder pressure as the first simulation trial of 14.4 atm. Opening a valve twice in one cycle requires camless valve operation. Available valve actuator technology was compared to the required valve actuation speed for this design and was determined to be feasible. Additionally, fuel injection timing was investigated regarding near-TDC injection. Fuel must be injected after the exhaust valve opens during the compression stroke to avoid fuel loss through the exhaust manifold. This late fuel injection was determined to be feasible based on previous Sandia National Laboratory injection-timing studies.

Contents

This document is dedicated to my parents and grandparents.

"Rejoice with your family in the beautiful land of life!"

-Albert Einstein

Acknowledgments

Special thanks to Dr. Frank Washko for serving as my thesis advisor during this process and to Dr. Rico Picone for providing the tools to compile this document. Thank you to Dr. Shawn Duan for serving on my thesis review committee.

Thank you to my family and friends who have supported me through this long journey.

Most importantly, I would like to thank God for blessing me with the ability to do this work and for guiding me in the process.

The following authors contributed to Abstract: Shelbie Davis and Frank Washko.

The following authors contributed to Introduction: Shelbie Davis and Frank Washko.

The following authors contributed to Chapter 1: Shelbie Davis and Frank Washko.

The following authors contributed to Chapter 2: Shelbie Davis and Frank Washko.

The following authors contributed to Chapter 3: Shelbie Davis and Frank Washko.

The following authors contributed to Chapter 4: Shelbie Davis and Frank Washko.

The following authors contributed to Conclusion: Shelbie Davis and Frank Washko.

The following authors contributed to AppendixA: Shelbie Davis and Frank Washko.

Listing of figures

The following document had been created to communicate the research conducted in the area of Variable Compression Ratio to meet the Mechanical Engineering Master's Thesis Requirements set by Saint Martin's University. The research was advised by Dr. Frank Washko and conducted by Shelbie L. Davis from 2016 to 2017.

0

Introduction

An automobile engine is a machine that transforms the chemical potential energy of fuel to rotational kinetic energy that powers a system, such as the drive train of an automobile, or similar. A gas vapor mixed with air is compressed in the engine cylinders and then ignited, resulting in a rapid expansion of the air/fuel mixture that pushes down on the piston used to intentionally compress

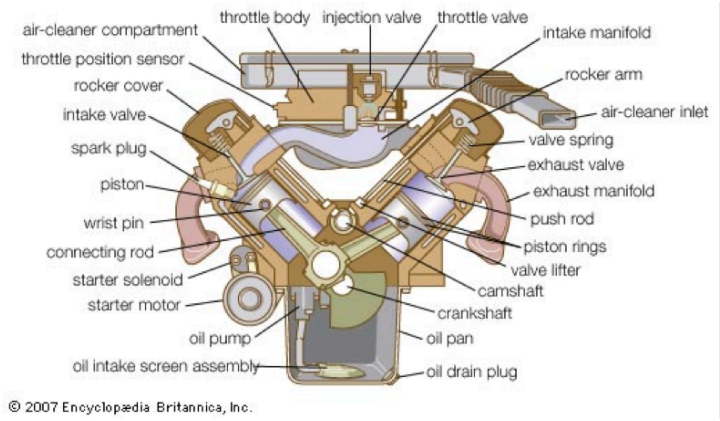

Figure 1: Engine Components

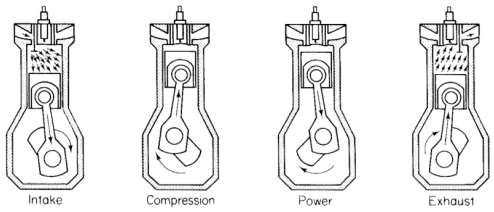

Figure 2: Four-Stroke Otto Cycle[7]

the air. The expansion force on the piston moves the piston downward, which turns the crankshaft outputting rotational kinetic energy. See Figure 1.

In a four-stroke engine there are four strokes (or stages) in one engine cycle. The first is the intake stroke. The intake valve is opened and the piston draws air into the cylinder. The compression stroke compresses air with both intake and exhaust valves closed. Before maximum compression, a fuel/air mixture is injected into the cylinder. The spark plug ignites the fuel and the expansion forces the piston down. The downward stroke due to expansion is called the power stroke and turns the crankshaft. The last stroke is the exhaust stroke in which the burned fuel and air mixture is forced out of the cylinder by the piston through the exhaust valve. See Figure 2.

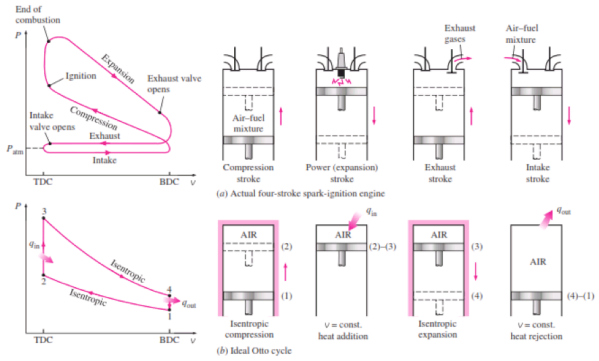

Figure 3: Real and Ideal Four-Stroke Otto Cycle [3]

The compression ratio of an Otto Cycle gas engine is dependent on the ratio between the volume of air in the cylinder at bottom dead center (BDC-lowest position of piston / larges volume of air in cylinder) and top dead center (TDC-highest position/smallest volume of air in the cylinder.) See equation (1) below.

$$r = \frac{V_{max}}{V_{min}} = \frac{v_1}{v_2} \tag{1}$$

By increasing the stroke of the engine (distance the piston travels), or decreasing the volume of the combustion chamber, the compression ratio will increase. Increasing the compression ratio will increase the thermal efficiency of the engine. This is true for ideal and real cycles[3]. See Figure 3. In the case of an Otto Cycle engine, ideal thermal efficiency is derived as solely a function of compression ratio r. The variable k is equal to the specific heat ratio $\frac{c_p}{c_v}$.

$$\eta_{th,otto} = 1 - \frac{1}{r^{k-1}} \tag{2}$$

The obstacle to overcome when increasing compression ratio is the issue of "knock." As the piston compresses the air, the temperature rises. The rise in temperature can result in auto combustion or "knock" meaning that the combustion of air-fuel mixture happens earlier than intended for proper combustion. This results are decreased power output, noise, and excess stresses that damages the engine.[5]

For different combinations of RPMs and load, the compression ratio can be knock-limited. For example, a specific RPM and load combination may limit the CR to 10. If the speed or load changes, the CR-limit might increase to 16 or 17. With traditional non-varying compression ratio designs, the engine runs with the lowest CR knock-limit which for this example would be 10. The high CRs at different speeds are not utilized. Variable compression ratios provide the ability to change the CR when the load and/or speed of the engine changes. This method increases the engine efficiency by taking full advantage of increased knock-limits. "A Comparative Study of Recent Advancements in the Field of Variable Compression Ratio Engine Technology" defines the benefits of a VCR engine as follows:

> "VCR engines can minimize possible risks of irregular combustion while optimizing brake specific fuel consumption toward higher power and torques."[5]

This explanation speaks to the previous discussion regarding the utilization of high CRs when able. The optimization of brake specific fuel consumption is an effect of this ability. The brake specific fuel consumption is a comparison factor used to compare engines based on how efficiently they converts fuel to work.[10] The term "brake" when referring to engine parameters denotes that the power output used in performance calculations includes friction loss. Indicated power is the total

power output of the engine not considering friction loss. Therefore, the following is true if *ihp* is indicated horsepower, *bhp* is brake horsepower, and *fhp* is friction-loss horsepower.[10]

$$ihp = bhp + fhp \tag{3}$$

By utilizing different compression ratios for different load/speed scenarios, the bsfc is optimized and the engine efficiency is increased.

Traditionally, compression ratio has been varied by changing the geometry of the combustion chamber during engine operation. The next section describes previous methods of geometry manipulation. Additionally, variable valve timing has been used to change the compression ratio as needed. This is done by closing and opening the exhaust and intake valves early or late. This strategy has allowed the engine to gain or lose approximately two compression ratio points (± 2)[8].

This study explores the ability to open the exhaust valve at the end of the compression stroke right before fuel injection to bleed off pressure allowing for an increased compression ratio beyond two additional points. By bleeding off pressure at the end of compression, uniform combustion is still present, but the volumetric change from TDC to BDC is large (CR17). If the pressure is not bled off, the engine may experience non-uniform combustion due to hotspots in the combustion chamber resulting in knock and damage to the engine.[12] In the compression stroke, temperature and pressure rise steadily until they both reach a high level possibly resulting in auto-ignition.[12] The spark plug also ignites the fuel-air mixture causing two zones of combustion. Due to rapid expansion in both areas, pressure oscillation occurs causing the knock phenomenon.[12]

1

Background

Harry Ricardo built the first VCR engine in the 1920s. His engine raised and lowered the cylinder and cylinder head with respect to the crankshaft.[4] VCR engines continued to be developed in the 20th and 21st centuries. Many different strategies for adjusting engine compression ratio were realized. Ford and Volvo investigated an adjustable piston that would change clearance volume and

therefore compression ratio. Ford patented a hydraulic piston design where the piston top was movable and controlled by engine oil pressure. The piston top extended to increase compression ratio. Mercedes also investigated the idea of a hydraulic piston. In 2000, Saab introduced an articulated cylinder head. One side of the cylinder head was attached to the crankcase with a hinge and could lift up to four degrees increasing cylinder volume. Saab claimed a compression ratio increase from 8:1 to 14:1 with this technology.[4] Peugeot developed a way to change the compression ratio by attaching the center of a rocker arm to the crankshaft. One end of the rocker arm was attached to the piston and the other end was attached to an intermediary gear. The intermediary gear engaged with a rack that was controlled by a hydraulic jack. This design raised and lowered the intermediary gear changing the length of the piston stroke. Waulis Motor Ltd. patented an "eccentric big end rod bearing"[4] which was an eccentric wheel on the connecting rod big end bearing. The eccentric wheel included a gear meshing with a ring gear.[4] This design changes the clearance volume at TDC. Gomecsys developed an eccentric crankshaft bearing. This invention basically consisted of a crankshaft bearing with eccentric wheels. By rotating the bearing wheels, the clearance volume at TDC changed.[4] Eccentric piston pins have also been developed for this same purpose. Nissan developed a multi-link rod-crank that involved an extra linkage between the crankshaft and connecting rod.[4] The extra linkage was connected to an actuator shaft that changes the compression ratio. Other patented designs have included extra chambers in the engine head[6] to increase or decrease compression. None of the designs mentioned above have been commercially produced for three main reasons – mechanical complexity, difficulty of control, and cost.[4] Currently, Nissan is close to breaking through the VCR commercial production glass ceiling with its plans for series production of its new VC-Turbo engine

initially introduced at the 2016 Paris Motor Show. It was debuted under the Infinity brand and features the lowering and raising of the piston at TDC. It uses the ”multi-link with actuator”[4] method to achieve a 8:1 to 14:1 compression ratio based on load.[8]

2

Concept and Procedure

2.1 Concept

Although Nissan is in the process of commercially producing a VCR engine, the engine gains only a few CR points from the "multi-link with actuator"[4] method. The simulation investigation in this paper provides a proof-of-concept that a greater CR gain is possible by opening the exhaust valve at

the end of the compression stroke. The two scenarios compared are as follows:

1. Engine simulation with CR 10 and traditional valve timing
2. Engine simulation with CR 17 and additional valve opening during compression

The goal is to achieve the same peak pressure in the combustion chamber for both scenarios. This is done by optimizing the additional valve opening timing during compression for the CR 17 scenario. If both scenarios achieve the same peak pressure, it will demonstrate the ability of an engine designed for a CR of 17 to "act" as a CR10 engine during RPM/load combinations that are knock-limited to 10. Ideally, changing the timing of the additional opening will allow the engine to run with a CR from 10 to 17 depending on RPM/load demand which will optimize bsfc.

2.2 Procedure

2.2.1 ANSYS Internal Combustion (IC) Engine Simulation

In the preliminary investigation, a Fluent-based IC Engine computational fluid dynamics (CFD) sliding mesh model was used to simulate the chamber pressure in an operating engine. Standard IC engine geometry provided by ANSYS was used including one set of inlet and outlet valves, engine head, and inlet and outlet ports. A cold flow simulation was performed, simulating a full engine cycle without combustion. The simulation was set to run from 0 degrees to 720 degrees crank angle. A control simulation with a set compression ratio of 10 and a standard valve timing profile (See Figure 2.1) provided cylinder pressure data in the form of a plot where the y-axis is cylinder pressure and the x-axis is degrees CA. The max output pressure (at TDC, compression stroke) was an important

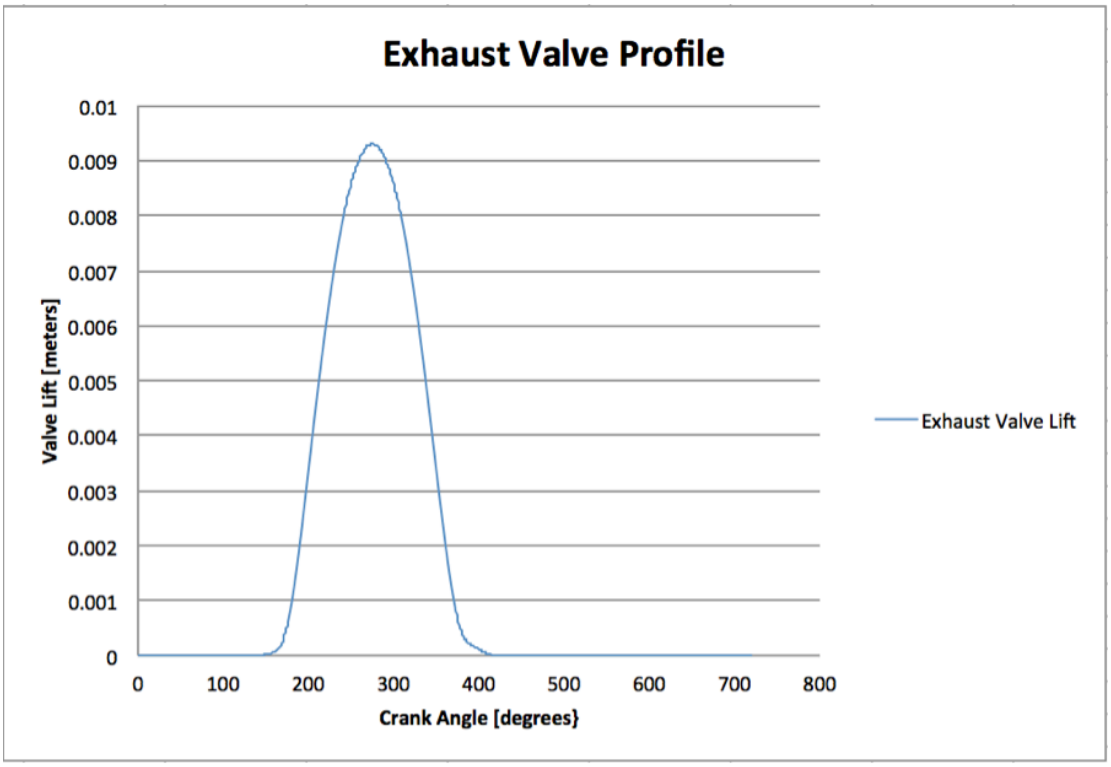

Figure 2.1: Traditional Exhaust Valve Profile

data point because the timing, duration, and magnitude of the additional valve opening during the compression stroke was dependent on the compression of max cylinder pressure. Unfortunately, IC Engine did not run a full cycle from 0 to 720 degrees to provide a full pressure plot. After discussing this issue with ANSYS support, it was advised to continue research using ANSYS Forte, the latest generation of engine simulation software.

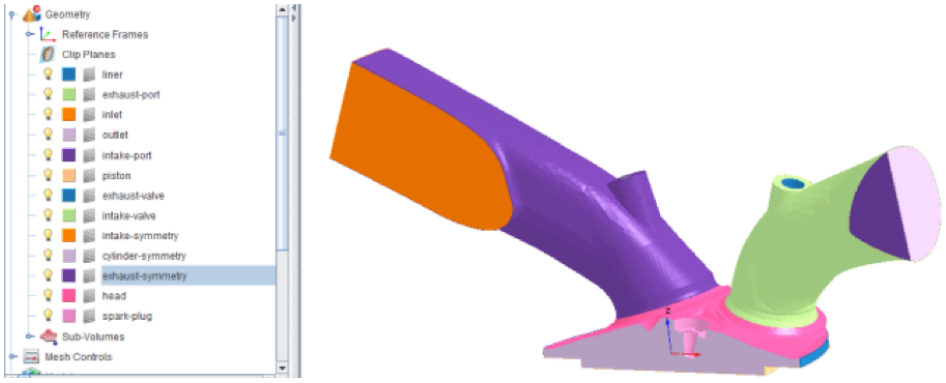

Figure 2.2: Engine Head in Forte [1]

2.2.2 Forte Simulation

A number of Forte Simulations were run for this research. This paper will primarily focus on three simulations – Test 5, Test 6, and Test 11. General settings for these simulations are shown in Table 2.1. The simulation process began with importing engine geometry as seen in Figure 2.2 and defining the appropriate mesh. Detailed settings can be viewed in Appendix A.

	CR 10 Simulation (Test 5)	CR 17 Simulation (Test 6)	CR 17 Simulation with Exhaust Valve Opening During Compression (Test 11)
Stroke	9.0 cm	15.48 cm	15.48 cm
Connecting Rod Length	14.43 cm	14.43 cm	14.43 cm
CR	10	17	17
Simulation Runs from	520 degrees to 880 degrees CA	520 degrees to 880 degrees CA	520 degrees to 880 degrees CA
RPM	2000	2000	2000
Cycle Type	4-Stroke	4-Stroke	4-Stroke
EVO	144 degrees	144 degrees	144 degrees625 degrees
EVC	419 degrees	419 degrees	419 degrees695 degrees
IVO	308 degrees	308 degrees	308 degrees
IVC	578 degrees	578 degrees	578 degrees
Exhaust Valve Duration Open	275 degrees	275 degrees	275 degrees70 degrees
Exhaust Valve Max Lift	9.3 mm	9.3 mm	9.3 mm1.77 mm
Intake Valve Duration Open	270 degrees	270 degrees	270 degrees
Intake Valve Max Lift	9.3 mm	9.3 mm	9.3 mm
SOI	700 degrees	700 degrees	700 degrees
EOI	718.4 degrees	718.4 degrees	718.4 degrees
Injection Duration	18.4 degrees	18.4 degrees	18.4 degrees
Max Cylinder Pressure	14.40744 atm	28.993 atm	14.439 atm

Table 2.1: Test 5 General Settings

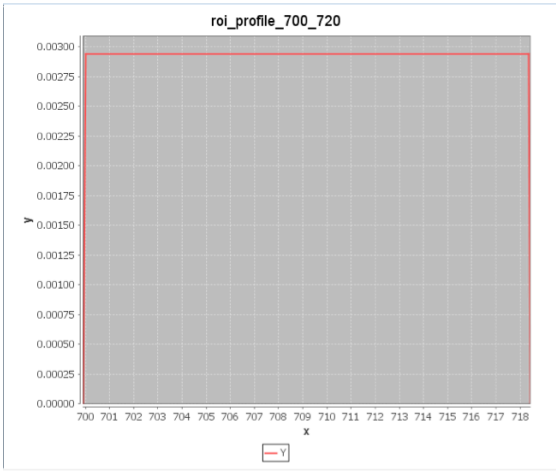

Figure 2.3: Fuel Injection Profile

Valve profiles which defined valve motion were imported as well as the fuel injection profile. See Figure 2.3. The intake and exhaust valve profiles were built in Excel format and imported into Ansys. The baseline exhaust valve lift profile is shown in Figure 2.1. The exhaust valve profile was changed after Test 6. The injection was set as a pulse injection beginning at 700 degrees CA with a 18.4-degree duration.

For the purpose of our research, a gasoline direct injection simulation was used. Direct injection is necessary in this concept, because the fuel must be injected near TDC at the end of the compression stroke to avoid fuel escaping when opening the exhaust valve during compression. That is, fuel can only be injected after the second exhaust event is finished. Port fuel injection would not be appropriate for this research because an air-fuel mixture is compressed, and thus would escape from the exhaust valve unburned during the second exhaust event.

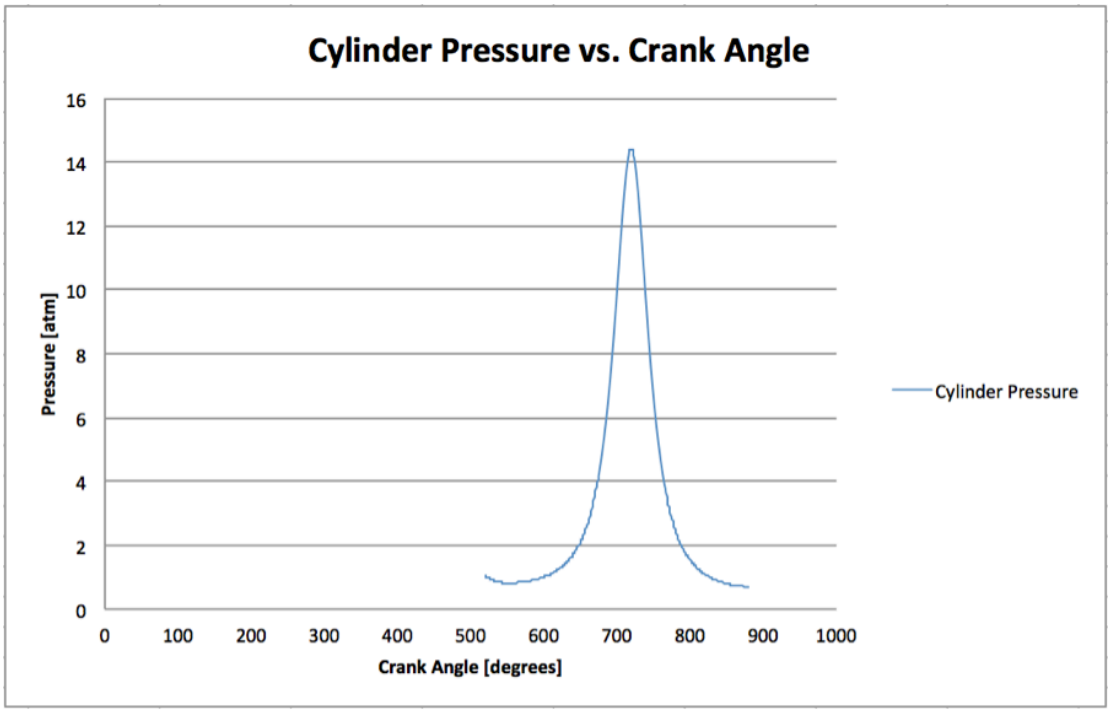

Figure 2.4: Cylinder Pressure Profile for CR10 with Traditional Valve Profile

2.2.3 Control Simulation - Test 5

"Test 5" was the first simulation trial that will be considered in this research. Test 5 used the settings listed in Table 2.1 including the valve profile seen in Figure 2.1 and a compression ratio of 10 (9.0 cm stroke). The valve had a max lift of 9.3 mm and began to open at 144 degrees CA. The maximum in-cylinder pressure for the Test 5 simulation was 14.40744 atm (1459.79 kPa). See Figure 2.4. This maximum pressure with a compression ratio of 10 was the "control" data point for the following simulation trials.

2.2.4 Simulation Modifications

NEW COMPRESSION RATIO: The simulation was changed to model the same situation as in Test 5 with the exception of increasing the Compression Ratio to 17 (See Table 2.1) . The following calculations represent how the Compression Ratio was recalculated:

- CR of 10 (Stroke = 9 cm)

$$V_{total} = 550.838 cm^3 \tag{2.1}$$

$$V_{cl} = 53.4634 cm^3 \tag{2.2}$$

$$V_{comp} = V_{total} - V_{cl} = 497.375 cm^3 \tag{2.3}$$

Solve for radius of cylinder,

$$V_{comp} = \pi * r^2 * stroke \tag{2.4}$$

- CR of 17 (Solve for new stroke[l])

$$CR = 17 = \frac{V_{tot2}}{V_{cl}} = \frac{V_{tot2}}{53.4634cm^3} \tag{2.5}$$

$$V_{tot2} = 908.878cm^3 \tag{2.6}$$

$$V_{comp2} = V_{tot2} - V_{cl} = 908.878cm^3 - 53.4634cm^3 = 855.414cm^3 \tag{2.7}$$

$$V_{comp2} = \pi * r^2 * l \tag{2.8}$$

$$V_{tot2} = 908.878cm^3 \tag{2.9}$$

$$V_{comp2} = V_{tot2} - V_{cl} = 908.878cm^3 - 53.4634cm^3 = 855.414cm^3 \tag{2.10}$$

$$V_{comp2} = \pi * r^2 * l \tag{2.11}$$

$$V_{comp2} = \pi * r^2 * l \tag{2.12}$$

$$855.414cm^3 = \pi * (4.19417cm)^2 * l \tag{2.13}$$

$$l = 15.4787cm \tag{2.14}$$

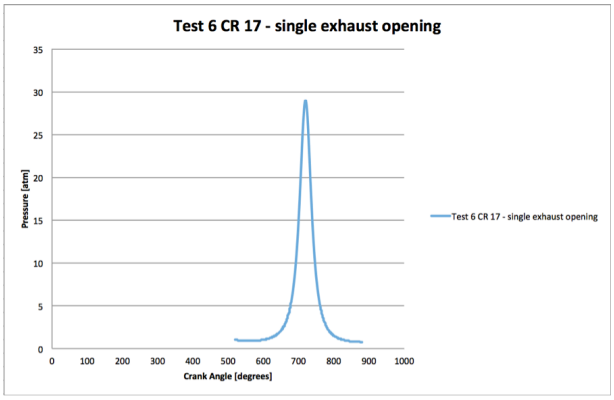

Figure 2.5: Cylinder Pressure Profile for CR17 with Traditional Valve Profile

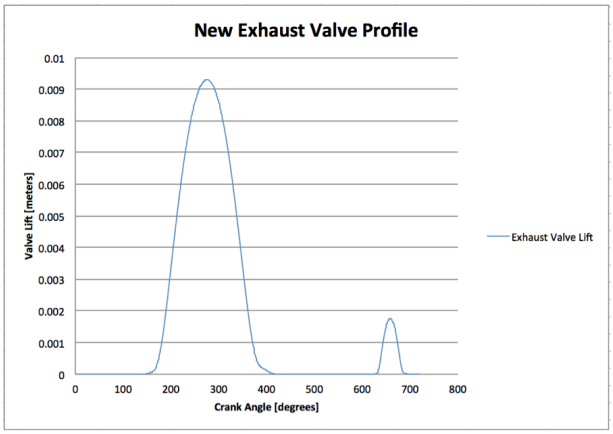

Figure 2.6: Exhaust Valve Profile with Opening During Compression Stroke

For Test 6, the stroke was changed to 15.4787 cm to achieve a Compression Ratio of 17. Test 6 ran this new compression ratio of 17 with the traditional valve profile displayed in Figure 2.1. The maximum pressure in the cylinder during the engine cycle was 28.993 atm (2937.72 kPa) as seen in Figure 2.5. Bleeding off some of the pressure during the compression stroke by changing the valve profile to include an extra exhaust opening was the next step in this investigation (Figure 2.6).

DEVELOPMENT OF EXHAUST VALVE COMPRESSION OPENING: In Test 5 and 6, the exhaust valve opened once during the exhaust stroke when the exhaust is forced out of the cylinder by the piston. In the following simulations after Test 5 and 6, the exhaust valve profile is modified to include a second opening during the end of the compression stroke. The new opening, which is shown as an additional "bump" on the plot in Figure 2.6, is developed from the initial opening profile and then moved along the x-axis to produce approximately the same maximum cylinder pressure as Test 5 (14.407 atm) but when the CR is 17. Maximum cylinder pressure is important because knock is dependent on cylinder pressure and air-fuel temperature. If CR 10 and CR 17 have the same maximum cylinder pressure, the engine can run with a significantly higher CR without hotspots occurring before combustion that can cause pre-ignition and non-uniform combustion resulting in knock.

The additional valve opening profile was calculated by scaling down the original opening that begins at 144 degrees CA. Use x_h to represent half of the valve opening duration meaning from the beginning of the valve opening to the peak of the valve opening. x_p is the crank angle at which the peak valve opening occurs. x_b is the crank angle at which the exhaust valve begins to open.

$$x_h = x_p - x_b = 275 \text{ degrees CA} - 144 \text{ degrees CA} = 131 \text{ degrees CA} \tag{2.15}$$

The duration from the beginning of the new opening to the peak of the new opening was chosen to be 25 degrees CA. Let x_n equal this duration. The following shows the percent of the new duration compared to the original x_h:

$$\frac{x_n}{x_h} * 100 = \frac{25}{131} * 100 = 19\% \tag{2.16}$$

The lift values (y-values) were multiplied by 19% to create the same profile shape but scaled by a factor of 19%. The final compression exhaust valve profile had duration of 70 degrees CA to avoid a sharp peak at the top of the profile curve.

The location along the x-axis for the new exhaust valve opening was initially arbitrary as long as it was after the exhaust valve opening during the exhaust stroke. After running the simulation with the additional opening, the maximum cylinder pressure was compared to the simulation with a CR of 10 (single exhaust valve opening). The initial placement of the new opening produced a cylinder pressure of 28.307 atm (2868.21 kPa). The new opening profile was then moved to the right in an attempt to arrive at the same maximum cylinder pressure of the CR 10 (14.407 atm). Many iterations of the simulation were run to finally match the maximum cylinder pressure. The progression of valve profiles from Test 5 though Test 11 is shown in Figure 2.7.

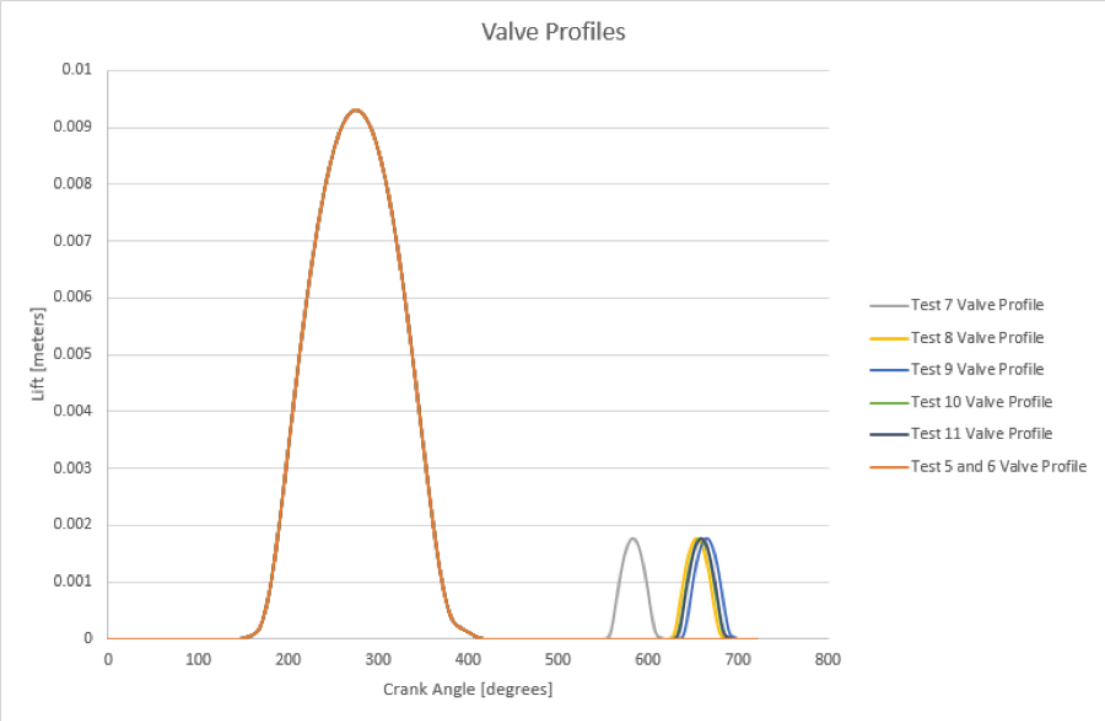

Figure 2.7: Progression of Exhaust Valve Profiles for Test 5 through Test 11

3

Results

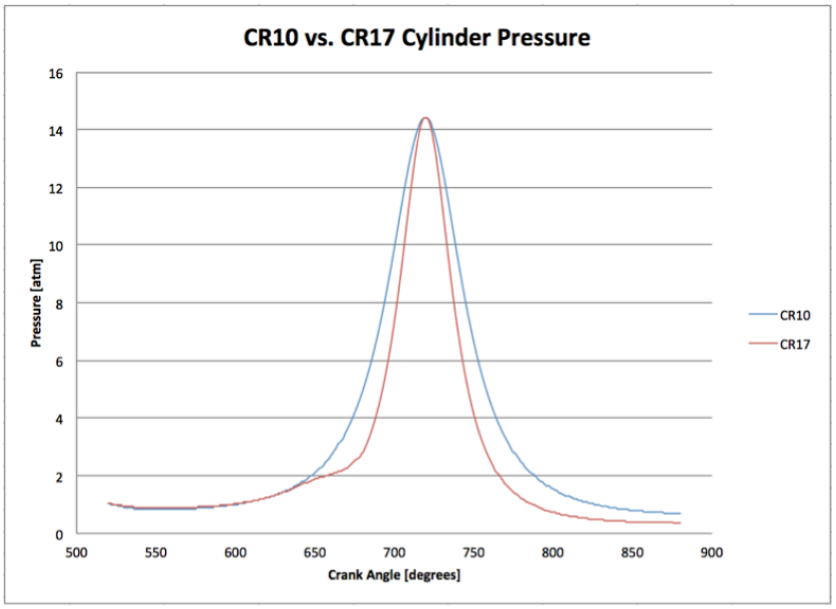

Figure 3.1: Test 5 (CR10) and Test 11 (CR17) Pressure Profile Comparison

The result of this research is if the exhaust valve is opened during compression at 625 degrees and closed at 695 degrees for a total of 5.833 ms at 2000 RPM, then the pressure in the combustion chamber is 14.439 atm (1463.03 kPa) for CR 17 which is virtually the same as the CR 10 maximum combustion chamber pressure of 14.407 atm (1459.79 kPa) as shown in Figure 3.1. See Table 3.1 for CR 10 and CR 17 comparison.

Parameter	CR10	CR17 w/ valve opening
Bore	8.39 cm	8.39 cm
Stroke	9.0 cm	15.48 cm
Exhaust Valve Open	144-419 degrees	144-419 degrees and 625-695 degree
Opening Duration (degrees)	275 degrees	275 degrees and 70 degrees
Opening Duration at 2000 RPM	22.92 ms	22.92 ms and 5.83 ms
Valve Lift	9.3 mm	9.3 mm and 1.77 mm
Valve Lift Speed at 2000 RPM	0.814278 mm/ms	0.814278 mm/ms and 0.606788 mm/ms
Fuel Injection	700-718.4 degrees	700-718.4 degrees
Max Cylinder Pressure	14.407 atm	14.439 atm

Table 3.1: Test 5 and Test 11 Results

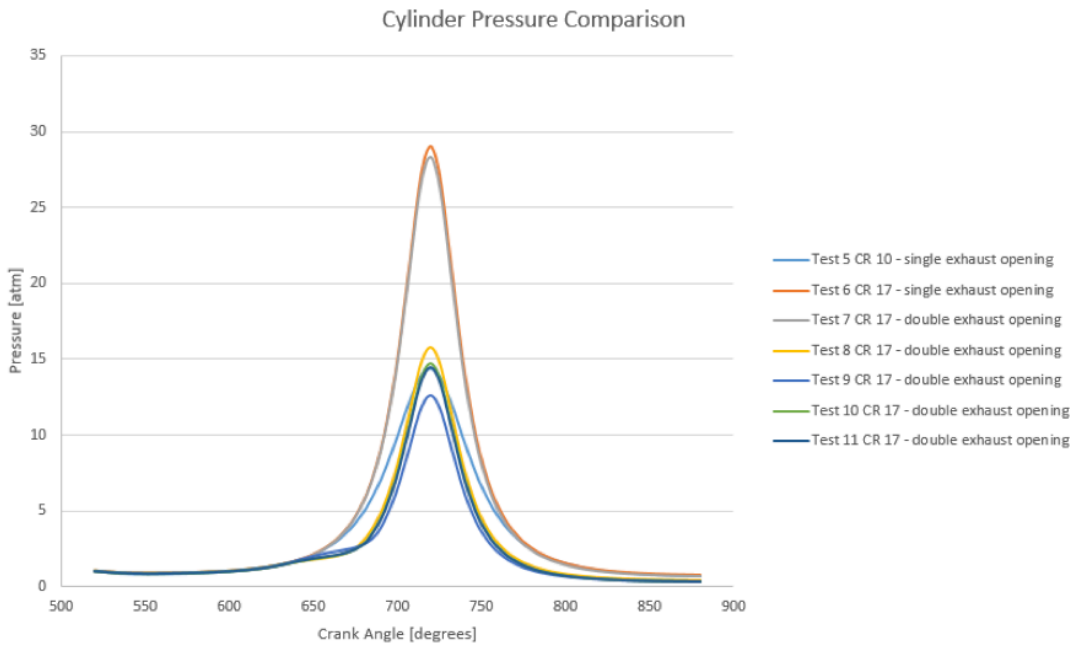

Figure 3.2: Cylinder Pressure Profiles for Test 5 though Test 11

Many simulations were required to reach the appropriate output pressure for CR 17 with an additional exhaust valve opening as shown in Figure 3.2. Moving the valve opening to the right on the x-axis (opening later in the cycle) reduced the output pressure. Comparing Test 6 with Test 7 indicates that when the valve opening was too close to the original opening (earlier in the compression stroke) and did little to reduce the cylinder pressure. Changing the duration or magnitude of the additional exhaust valve opening profile could provide flexibility in placement of the additional opening on the x-axis. RPM will also change the placement of the additional exhaust opening. For the scope of this investigation, RPM was assumed constant at 2000 and a specific valve profile was chosen to serve as a proof-of-concept.

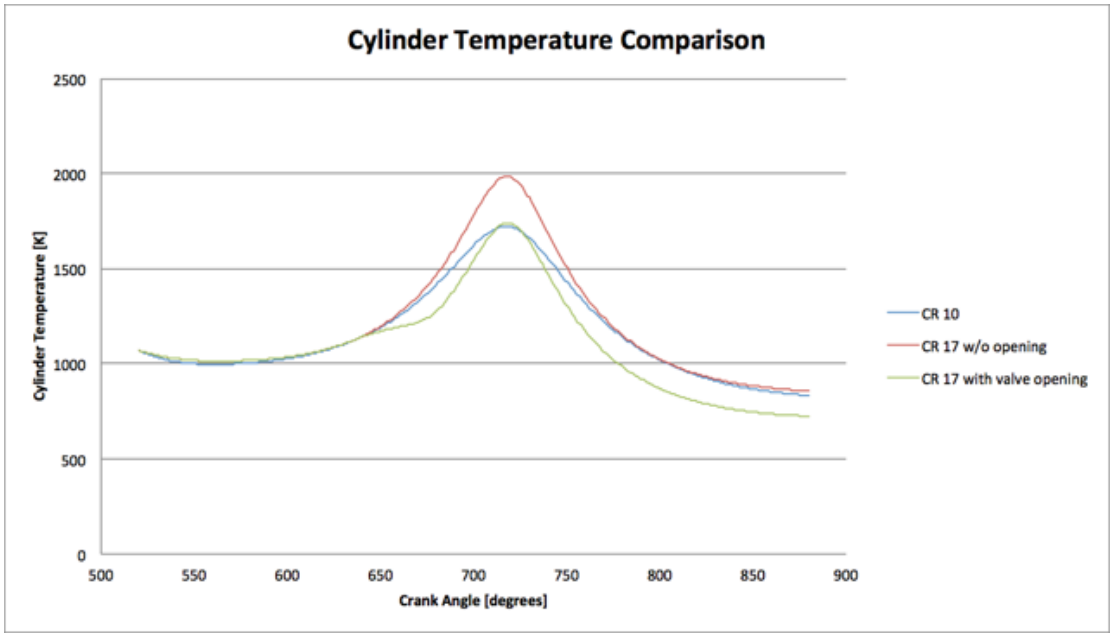

Figure 3.3: Cylinder Temperature Comparison for Tests 5, 6, and 11

It is important to note in Figures 2.4, 2.5, 3.2, 3.1, and 4.1 that the max pressure does not increase further after TDC because the combustion portion of this simulation is turned off. The max pressure output models a "cold flow" cycle meaning without combustion. Although this is a "cold flow" cycle, it is important to note that the temperature increase due to only compression is virtually the same for Test 5 and Test 11. See Figure 3.3. This indicates that bleeding off pressure at the end of the compression stroke not only allows the CR17 with an extra valve opening to "act" like the CR 10 with regard to cylinder pressure but also with regard to cylinder temperature.

This idea of opening the exhaust valve during the compression stroke of an engine is intended for a camless engine. This must be considered because traditional valve cams have only one cam lobe. Adding another valve opening in one cycle will require two lobes on the same cam in a traditional

valvetrain. This unusual profile is likely not feasible; therefore, an additional valve opening during the compression stroke would need to be done with an electro-magnetic actuator (EMV), an electro-hydraulic actuator (EHV), or an electro-pneumatic actuator (EPV).

3.0.1 Efficiency

The following equation is used to calculate the average ideal efficiency for Test 5 (CR 10) and Test 6 (CR 17 with traditional exhaust opening) by using values of c_p and c_v through the cycle form 520 to 880 degrees CA and the appropriate CR:

$$\eta_{th,otto} = 1 - \frac{1}{r^{k-1}} \text{ where } k = \frac{c_p}{c_v} \text{ and } r = CR \tag{3.1}$$

For CR 10 the average ideal efficiency is as follows:

$$\eta_{th,otto} = 48.16\% \tag{3.2}$$

For CR 17 the average ideal efficiency is as follows:

$$\eta_{th,otto} = 55.23\% \tag{3.3}$$

These two efficiencies indicate the minimum and maximum average ideal efficiency possible when varying the CR from 10 to 17.

4

Discussion

After manipulating the compression exhaust valve location many times, the maximum cylinder pressure of 14.439 atm was achieved for CR 17 with an additional valve opening during compression. This is compared with the original CR 10 traditional valve profile simulation maximum pressure of 14.407 atm. For the crank angle resolution of this simulation, CR17 comes within 0.22% of CR 10.

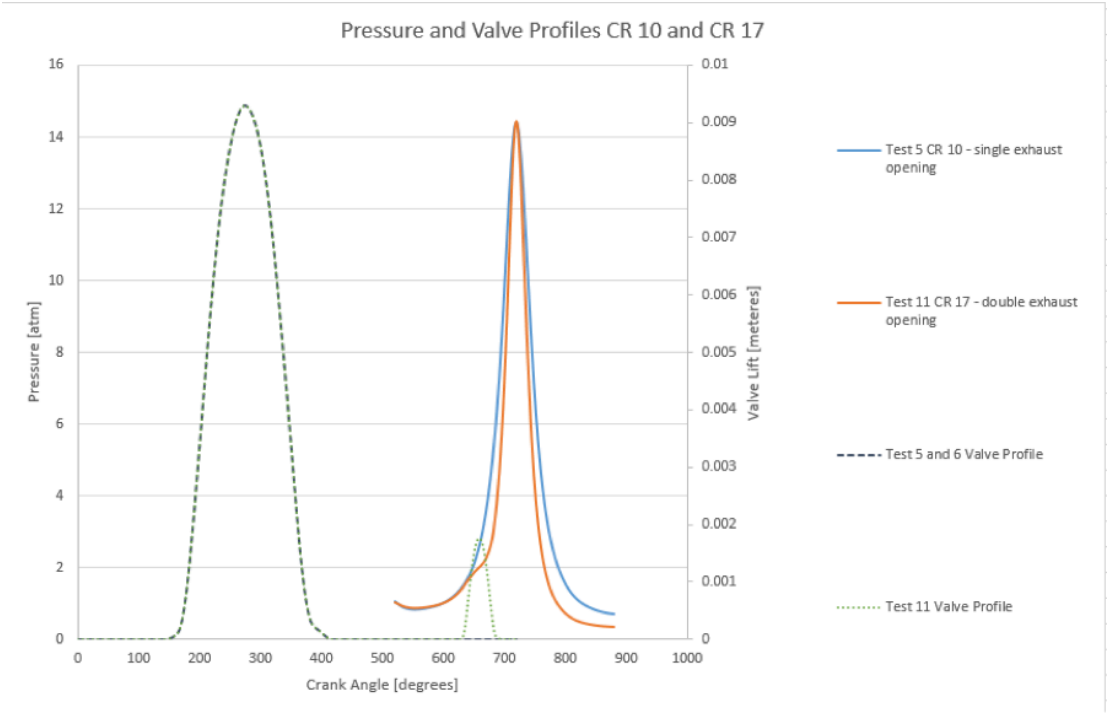

Figure 4.1: Valve Profiles and Pressure Profiles of Test 5 and Test 11

Figure 3.1 shows the pressure profile comparison between Test 5 (CR 10) and Test 11 (CR 17). Test 11 produced a pressure profile that virtually matched Test 5 but had a smaller spread along the x-axis. Through examination of Figure 4.1, it can be concluded that the valve opening during the compression stroke delays rapid compression until slightly later in the cycle which produces the difference in slope for CR 10 and CR 11 from 626 CA to peak pressure at 720 CA. It can be concluded that Test 11 with a CR of 17 produced an equivalent maximum cylinder pressure to Test 5 with a CR of 10 demonstrating the ability of the engine to run with an increased compression ratio while avoiding the knock-limitation of certain RPM/load combinations.

4.0.1 Feasibility

Two main considerations must be analyzed to evaluate the feasibility of opening the exhaust valve during the end of the compression stroke to avoid knock and increase efficiency. First, the ability of a valve to be opened twice in one cycle, in the required amount of time, must be investigated. Second, the fuel must be injected after the second exhaust vale opening.

Valve Parameter	Values
EVO During Exhaust Stroke	144 degrees
EVC During Exhaust Stroke	419 degrees
EVO During Compression Stroke	625 degrees
EVC During Compression Stroke	695 degrees
SOI	700 degrees
EOI	718.4 degrees
Max Lift During Exhaust Stroke	9.33 mm
Max Lift During Compression Stoke	1.77 mm
Valve Lift Speed Required for Exhaust Stroke Valve Opening at 2000 RPM	0.814278 mm/ms
Time from valve fully closed to valve fully open during Exhaust Stroke @ 2000 RPM	11.46 ms
Total time valve open during Exhaust Stroke @ 2000 RPM	22.92 ms
Valve Lift Speed Required for Compression Stroke Valve Opening at 2000 RPM	0.606788 mm/ms
Time from valve fully closed to valve fully open during Compression Stroke @ 2000 RPM	2.915 ms
Total time valve open during Compression Stroke @ 2000 RPM	5.83 ms

Table 4.1: Valve Parameters

VALVE OPENING SPEED FEASIBILITY: As stated in a previous section, the concept of opening the exhaust valve during the compression stroke is meant for a camless engine. Camless Variable Valve Actuation (VVA) has been developing in recent years and can be divided into electro-magnetic, electro-hydraulic, and electro-pneumatic actuation.[9] An electro-hydraulic prototype for variable valve-timing was developed at Michigan State University and Published by SAE in 2013.[9] The valve produced an opening and closing time of approximately 3 ms. Fully-opened life was 10 mm. Mag-

netic valve actuators produced by MMT take 2.8 ms for an 8 mm lift.[2] These magnetic valve actuators are used for engine valve operation and are an example of ultra fast valve actuators currently produced. Using the Exhaust Valve Opening data in Table 4.1 the following calculations are produced:

For exhaust valve exhaust opening,

$$dx = 9.33 \text{ mm} \tag{4.1}$$

$$dt = \frac{0.5 * (419 - 144) \text{ degrees}}{1} * \frac{1 \text{ rev}}{360 \text{ degrees}} * \frac{1 \text{ min}}{2000 \text{ rev}} * \frac{60000 \text{ ms}}{1 \text{ min}} = 11.458 \text{ ms} \tag{4.2}$$

$$\frac{dx}{dt} = \frac{9.33 \text{ mm}}{11.458 \text{ms}} = 0.814278 \frac{\text{mm}}{\text{ms}} \tag{4.3}$$

For exhaust valve compression opening,

$$dx = 1.77 \text{ mm} \tag{4.4}$$

$$dt = \frac{0.5 * (695 - 625) \text{ degrees}}{1} * \frac{1 \text{ rev}}{360 \text{ degrees}} * \frac{1 \text{ min}}{2000 \text{ rev}} * \frac{60000 \text{ ms}}{1 \text{ min}} = 2.917 \text{ ms} \tag{4.5}$$

$$\frac{dx}{dt} = \frac{1.77 \text{ mm}}{2.917 \text{ ms}} = 0.606788 \frac{\text{mm}}{\text{ms}} \tag{4.6}$$

For Michigan State valve,

$$\frac{dx}{dt} = \frac{10 \text{ mm}}{2.9 \text{ ms}} = 3.44828 \frac{\text{mm}}{\text{ms}} \tag{4.7}$$

For MMT valve,

$$\frac{dx}{dt} = \frac{8 \text{ mm}}{2.8 \text{ ms}} = 2.85714 \frac{\text{mm}}{\text{ms}} \tag{4.8}$$

The valve profile in this paper requires significantly slower valve actuation than available technology as shown at Michigan State and MMT (See Table 4.2); therefore, this valve profile can be considered feasible regarding valve actuation even at RPMs above 2000.

Valve	Speed
Valve Lift Speed Required for Exhaust Stroke Valve Opening at 2000 RPM	0.814278 mm/ms
Valve Lift Speed Required for Compression Stroke Valve Opening at 2000 RPM	0.606788 mm/ms
Michigan State Hydraulic Valve	3.44828 mm/ms
MMT Magnetic Valve	2.85714 mm/ms

Table 4.2: Valve Actuation Speed Comparison

VALVE OPENING VS. FUEL INJECTION TIMING FEASIBILITY: The other consideration when opening the exhaust valve during compression is preventing injected fuel from escaping the cylinder when the pressure is bled off. The fuel must be injected after the exhaust valve is closed

during compression. For Test 11, the valve is fully closed at 695 CA degrees. TDC is at 720 CA degrees for this simulation. Stratified charge engines inject fuel just before ignition. This injection type should be used when opening the exhaust valve during ignition to avoid fuel from being bled off with the pressurized air. Based on research done by Sandia National Laboratories,[11] stratified charge direct injection spark ignition (DISI) can inject fuel as late as 23 degrees bTDC when running on E85 fuel compared to 31 degrees bTDC running on gasoline. This research indicates that it is possible to inject fuel after 695 CA degrees. Further research in opening the exhaust valve during combustion should be focused on moving the opening earlier in the compression stroke by changing the opening duration and magnitude. Closing the exhaust valve before 695 CA degrees, will avoid feasibility issues with near-TDC fuel injection.

5

Conclusion

It can be concluded from the research conducted, that the compression ratio of a four-stroke, direct-injection, combustion engine can be varied by opening the exhaust valve during the compression stroke before fuel is injected. By using this method, a compression ratio of at least 17 can theoretically be achieve for load and RPM parameters that allow for a higher knock-limit. With this

design, an engine could possibly be designed for a mechanical compression ratio of 17 but "act" as a CR 10 engine by bleeding off pressure before TDC for specific load-RPM parameters that require a lower compression ratio due to knock. This design should allow the engine to operate anywhere between CR10 and CR17 depending on the knock-limit.

It can also be concluded based on the previous discussions that this design is feasible regarding valve actuation speed and fuel injection timing. Currently, there are valve actuators that will satisfy the valve speed requirement of this VCR 17 design. Drawing from research done by Sandia National Laboratory,[11] it is also feasible to inject fuel, specifically E85, near-TDC which satisfies the exhaust valve opening requirements.

It is advised that further research on this topic should include varying RPM and changing the exhaust valve compression profile with regard to duration and magnitude. Changing these variables may allow the exhaust valve to be opened earlier in the compression stroke permitting earlier fuel injection timing. Possible cam profiles or camless valve actuator technology may be paired further with this research to produce an engine prototype utilizing the compression exhaust valve profile.

6

Appendix A: Forte Simulation Settings

Four files from ANSYS were used and are listed in Table 6.1:

File Type	File Name
Engine Geometry File	Forte_GDI.stl
Exhaust Valve Profile File	exhaust_valve_lift.csv
Intake Valve Profile File	intake_valve_lift.csv
Data Output File	spacial_output.csv

Table 6.1: ANSYS Files

The geometry file included geometry faces as seen in Figure 2.2. The geometry faces and their descriptions are listed in Table 6.2.

Geometry	Description
Liner	Vertical perimeter of cylinder head
Exhaust Port	Exhaust air flows through this port out of cylinder during the exhaust stroke
Intake	Face at beginning of intake port oriented perpendicular to air flow through intake port
Outlet	Face at end of exhaust port oriented perpendicular to exhaust flow through exhaust port
Intake-port	Intake air flows through this port into cylinder during the intake stroke
Piston	Located directly below cylinder head. Looks like bottom of cylinder head in 2.2
Exhaust-valve	Unable to see in refForteEng but is the valve that opens and closes to let exhaust out of cylinder to flow through exhaust port
Intake-valve	Unable to see in refForteEng but is the valve that opens and closes to let intake air into cylinder
Intake-symmetry	Flat, vertical face of symmetry for intake port
Cylinder-symmetry	Flat, vertical face of symmetry for engine head
Exhaust-symmetry	Flat, vertical face of symmetry for exhaust port
Head	Engine head walls
Spark Plug	Geometry for spark plug

Table 6.2: ANSYS Geometry

From these geometry walls, five walls were selected to create a subvolume – cylinder-symmetry, head, liner, piston, and sparkplug. This subvolume was titled "chamber" and represents the region of interest within the cylinder to be analyzed. The mesh for the chamber is set up as an adaptive mesh refinement, which is active between 700 and 800 degrees CA to improve resolution on the temperature data during combustion. (Note: Combustion is turned off for simulaitons discussed in paper.) The "Solution Adaptive Meshing" function is used to achieve this. The following settings in

Table 6.3 were used in the "Solution Adaptive Meshing" setting.

Setting Type	Setting
Title	SAM-Temperature
Quantity Type	Gradient of Solution Field
Solution Variables	Temperature
Bounds Option	Statistical
Sigma Threshold	0.5
Size as fraction of Global Size	1/4
Active Between	700 and 800 degrees CA
Sub-Volume	Chamber

Table 6.3: Adaptive Mesh Settings for Temperature

Solution Adaptive Meshing was also used for higher resolution velocity data for the entire domain. See Table 6.4.

Setting Type	Setting
Title	SAM-Velocity
Quantity Type	Gradient of Solution Field
Solution Variables	VelocityMagnitude
Bounds Option	Statistical
Sigma Threshold	0.5
Size as fraction of Global Size	1/2
Active	Always
Sub-Volume	Entire Domain

Table 6.4: Adaptive Mesh Settings for Velocity

Geometry walls were then meshed with settings listed in Table 6.5[1].

Name	Location	Refinement Type	Size Fraction	Cell Layers	Active
Wall	Cylinder-symmetry, exhaust-symmetry, intake-symmetry, exhaust-port, intake-port, head, piston, liner, spark-plug	Surface	1/2	1	Always
Wall	Inlet, outlet	Surface	1/2	2	Always
Spark	0.551, 0.0945, 0.1678	Point (radius = 0.6 cm)	1/4	N/A	Always
Valves	Exhaust-valve, intake-valve	Surface	1/4	2	Always
Tdc1	Head, piston, liner	Surface	1/4	2	340-380 CA
Tdc2	Head, piston, liner	Surface	1/4	2	700-740 CA
Chamber	Chamber	Secondary volume	1/2	N/A	Always

Table 6.5: Geometry Mesh Settings

Chemistry of the gasoline was imported from the ANSYS Forte data directory, which models basic gasoline chemistry. The flame speed was specified with a turbulent flame speed ratio of 1.2. The default k-epsilon turbulence model was used. A solid cone injection setting was used with a mass fraction of 1.0. It was modeled as a pulsed injection with a droplet density of 1. The inflow droplet temperature was 400K. The fuel was injected with a constant discharge coefficient and angle, 0.7 and 14 degrees respectively. The drop size distribution was 3.5 and the shape parameter was 120 microns in diameter. Additional settings are listed in Table 6.6.

Setting Type	Settings
Size Constant of KH Breakup	0.5
Time Constant of KH Breakup	10
Critical Mass Fraction for New Droplet Generation	0.03
SMR Conservation in KH Breakup	Activated
Size Constant of RT Breakup	0.1
Time Constant of RT Breakup	1.0
RT Distance Constant	1.9
Gas Environment Constant	0.5

Table 6.6: Fuel Settings

The injection was set as a pulse injection beginning at 700 degrees CA with a 18.4-degree duration. The injection profile titled "roi_profile_700_720.csv" was used to define these injection-timing settings. See Figure 2.3. The injection location and direction are listed in Table 6.7.

Nozzle 1	X	Y	Z
Location	-5.296 mm	0.634 mm	6.468 mm
Direction	3.0415 mm	2.73735 mm	-9.12449 mm
Nozzle 2	X	Y	Z
Location	-5.65 mm	1.1885 mm	6.5991 mm
Direction	1.49781 mm	5.08692 mm	-8.4782 mm
Nozzle 3	X	Y	Z
Location	-6.7647 mm	0.72441 mm	6.1653 mm
Direction	-2.9025 mm	2.74977 mm	-9.16592 mm

Table 6.7: Nozzle Injection Settings

Boundary Conditions were defined for the Inlet in Table 6.8.

Inlet Boundary Conditions	Settings
Location	Pressure_In
Inlet Type	Pressure Inlet
Constant Pressure	8E+04 Pa
Mass Fraction O_2	0.233
Mass Fraction N_2	0.767
Turbulent Kinetic Energy	100000 $\frac{cm^2}{sec^2}$
Length Scale	1 cm

Table 6.8: Inlet Boundary Conditions

Boundary Conditions were defined for the Outlet in Table 6.9.

Outlet Boundary Conditions	Settings
Location	Pressure_Out
Outlet Type	Pressure Outlet
Outlet Pressure	1E+05 Pa
Offset Distance to Apply Pressure	0.0 cm
Turbulent Kinetic Energy	10000 $\frac{cm^2}{sec^2}$
Length Scale	1 cm

Table 6.9: Outlet Boundary Conditions

Boundary Conditions were defined for the Piston in Table 6.10.

Piston Boundary Conditions	Settings
Location	Piston
Constant Temperature	485 K
Motion Type	Slider-Crank Model
Stroke	9.0 cm
Connecting Rod Length	14.43 cm
Piston Offset	0.0 cm
Movement Type	Moving Surface
Direction	Z-direction
Z	1.0

Table 6.10: Piston Boundary Conditions

Boundary Conditions were defined for the Intake in Table 6.11.

Intake Boundary Conditions	Settings
Location	Intake-port
Constant Temperature	313 K

Table 6.11: Intake Boundary Conditions

Boundary Conditions were defined for the Exhaust in Table 6.12.

Exhaust Boundary Conditions	Settings
Location	Exhaust-port
Constant Temperature	485 K

Table 6.12: Exhaust Boundary Conditions

Boundary Conditions were defined for the Liner in Table 6.13.

Liner Boundary Conditions	Settings
Location	Liner
Constant Temperature	500 K
Head	Setting
Location	Head
Constant Temperature	485 K

Table 6.13: Liner Boundary Conditions

Boundary Conditions were defined for the Intake Valve in Table 6.14.

Intake Valve Boundary Conditions	Settings
Location	Intake-valve
Heat Transfer	Activated
Temperature	400 K
Motion Type	Offset Table
Direction	X=0.241922 cm, Y=0.0 cm, Z=-0.970296 cm
Intake take valve motion file	Intake_valve_lift.csv
Valve Motion Activation Threshold	0.02 cm
Approx. Cells in Gap at Min. Lift	1.5

Table 6.14: Intake Valve Boundary Conditions

Boundary Conditions were defined for the Exhaust Valve in Table 6.15.

Exhaust Valve Boundary Conditions	Settings
Location	Exhaust-valve
Temperature	777 K
Motion Type	Offset Table
Vertices to Transform	Interior
Direction	X=-0.327218 cm, Y=0.0 cm, Z=-0.944949 cm
Exhaust Valve Motion File	Exhaust_valve_lift.csv
Valve Motion Activated Threshold	0.02 cm
Approx. Cells in Gap at Min. Lift	1.5

Table 6.15: Exhaust Valve Boundary Conditions

Boundary Conditions were defined for the Symmetry in Table 6.16.

Symmetry Boundary Conditions	Settings
Location	Cylinder-symmetry, exhaust-symmetry, and intake-symmetry

Table 6.16: Symmetry Boundary Conditions

Boundary Conditions were defined for the Spark Plug in Table 6.17.

Spark Plug Boundary Conditions	Settings
Location	head
Temperature	485 K

Table 6.17: Spark Plug Boundary Conditions

Spark ignition timing settings are listed in Table 6.18.

Spark Ignition Timing	Settings
Kernel Flame to G-Equation Switch Constant	2.0 mins
Kernel Radius for Kernel to G-equation	0.1 cm
Flame Development Coefficient	0.5
Number of Flame Particles for Each Spark Plug	3000
Location	X=0.551 cm, Y=0.0945 cm, Z=-0.1678 cm
Starting Angle	705.0 CA degrees
Duration	10.0 CA degrees
Energy Release Rate	20.0 J/sec
Energy Transfer Efficiency	0.5
Initial Kernel Radius	0.25 mm

Table 6.18: Spark Ignition Timing Settings

Default Initialization Settings are listed in Table 6.19.

Default Initialization	Settings
Initialization Order	2
Phi	1.0
EGR Fraction	0.0
Internal EGR	Estimate from CR
CR	10
Composition	Exhaust_gas
Temperature	1070 K
Pressure	1.05459E+05 Pa
Turbulent Kinetic Energy	10000 $\frac{cm^2}{sec^2}$
Length Scale	1.0 cm
Velocity Components	All values set to zero

Table 6.19: Initialization Settings

Intake Initialization Settings are listed in Table 6.20.

Intake Initialization	Settings
Location	X=-5.6838, Y=1.4295, Z=4.2858 cm
Initialization Order	1
Temperature	313 K
Pressure	8.0E+04 Pa
Turbulent Kinetic Energy	10000 $\frac{cm^2}{sec^2}$
Length Scale	1.0 cm

Table 6.20: Intake Initialization Settings

Exhaust Initialization Settings are listed in Table 6.21.

Exhaust Initialization	Settings
Location	X=4.7892, Y=1.5061, Z=3.1552 cm
Initialization Order	3
Composition	Exhaust_gas
Temperature	1070 K
Pressure	1.0E+05 Pa
Turbulent Kinetic Energy	10000 $\frac{cm^2}{sec^2}$
Length Scale	1.0 cm

Table 6.21: Exhaust Initialization Settings

Simulation Controls are listed in Table 6.22.

Setting Type	Settings
Simulation Runs from	520 degrees to 880 degrees CA
RPM	2000
Cycle Type	4-Stroke
Initial Simulation Time Step	5.0E-7 seconds
Max. Crank Angle Delta Per Time Step	1.1 degrees
Max. Time Step Option	Constant
Max. Simulation Time Step	1.0E-5 sec

Table 6.22: Simulation Control Settings

Other Default Settings are listed in Table 6.23.

Other Defaults	Settings
Time Step Growth Factor	1.3
Fluid Acceleration Factor	0.5
Rate of Strain Factor	0.6
Convection Factor	0.2
Internal Energy Factor	1.0
Max. Convection Subcycles	8

Table 6.23: Other Default Settings

Chemistry Solver Default Settings are listed in Table 6.24.

Chemistry Solver Defaults	Settings
Absolute Tolerance	1.0E-12
Relative Tolerance	1.0E-5

Table 6.24: Chemistry Default Settings

Dynamic Cell Clustering Settings are listed in Table 6.25.

Dynamic Cell Clustering	Settings
Max Temperature Dispersion	10 K
Max. Equilibrium Ratio Dispersion	0.05

Table 6.25: Dynamic Cell Clustering Settings

Output Controls Settings are listed in Table 6.26.

Setting Type	Settings
Spatially Resolved Crank Angle Output Control	Every 10 degrees CA
User Defined Output control	Spatial_output.csv
Solutions per Results File	1
Spatially Averaged Crank Angle Output Control	Every 1 degree

Table 6.26: Output Controls Settings

References

[1] (2017). Ansys internal combustion engines tutorial guide 2017. web.

[2] (2017). Fast actuator, control valve actuator for valve actuation mmt. web.

[3] Cengel, Y. A. and Boles, M. A. (2011). *Thermodynamics: An Engineering Approach*. McGraw-Hill, 7 edition.

[4] Council, N., Sciences, D., Systems, B., and Committee on the Assessment of Technologies for Improving Fuel Economy of Light-Duty Vehicles, P. (2015a). *Appendix O*. National Academies Press.

[5] Council, N., Sciences, D., Systems, B., and Committee on the Assessment of Technologies for Improving Fuel Economy of Light-Duty Vehicles, P. (2015b). *Chapter 2*. National Academies Press.

[6] Cronstedt, V. (1969). Variable compression ratio piston assembly. US Patent 3,450,111.

[7] Flagan, R. C. and Seinfeld, J. H. (2012). *Fundamentals of air pollution engineering*. Dover Publ.

[8] Kendall, J. (2016). Nissan unveils 2018 production variable-compression-ratio ice.

[9] Lou, Z. D., Deng, Q., Wen, S., Zhang, Y., Yu, M., Sun, M., and Zhu, G. (2013). Progress in camless variable valve actuation with two-spring pendulum and electrohydraulic latching. *SAE Int. J. Engines*, 6:319–326.

[10] Obert, E. F. (1973). *Internal combustion engines and air pollution: based on Internal combustion engines, 3d ed.* Intext Educational Publishers, 3 edition.

[11] Sjöberg, M., Zeng, W., Reuss, D., Zhao, R., Egolfopoulos, F., Mehl, M., and Pitz, W. (2013). Sae/ksae 2013 international powertrains, fuels and lubricants meeting. In *Characterization of Spray-guided DISI Engine Combustion with near-TDC Injection of E85 using High-Speed Imaging, Spectroscopy, Flame Measurements and Modeling*. ENERGY EFFICIENCY AND RENEWABLE ENERGY: Sandia National Laboratories.

[12] Wang, Z., Liu, H., and Reitz, R. D. (2017). Knocking combustion in spark-ignition engines. *Progress in Energy and Combustion Science*, 61:78 – 112.